CHAPTER 6

Modeling the effect of a glucagon challenge on glucose homeostasis in humans

M.G.J. van Dongen[1], R. Alvarez-Jimenez[1], J. Stevens[1], L.A. Peletier[2], A.F. Cohen[1], J. Burggraaf[1]

1. Centre for Human Drug Research (CHDR), Leiden, The Netherlands
2. Mathematical Institute, Leiden University, Leiden, The Netherlands

ABSTRACT

Modeling glucose metabolism is challenging because of the complex interactions between the hormones involved and the simultaneous effect on glucose in the system. This is particularly true for models incorporating the contribution of glucagon to glucose homeostasis; in fact models incorporating modulation the glucagon receptor have not been described yet. Therefore we have developed a semi-mechanistic model to describe the glucagon-insulin-glucose homeostasis in 36 healthy subjects during a glucagon challenge. Briefly, this challenge consisted of a 3 hrs infusion of somatostatin to block endogenous release of insulin and glucagon with simultaneous infusion of high dose glucagon and physiological dose insulin. The model captured glucagon and glucose dynamics, including the amplifying effects of glucagon on hepatic glucose production with the magnitude of the effect being dependent on the prevailing insulin concentration. Glucagon production was inhibited by elevated glucose concentrations. We observed a rapid increase of the glucose concentration in response to glucagon followed by a slow decrease in the HGP, which is consistent with the internalization of glucagon receptors (GCGR) upon stimulation by glucagon, which was captured by incorporating an effect compartment. The model also captured the effects of glucose on insulin production and the insulin-independent and insulin-dependent effect on glucose elimination.

This model, based on glucagon challenge data, could contribute to a better understanding of pathophysiology of diabetes mellitus. It describes the general trend and can therefore serve as a basis for drug development. Furthermore, an extension of this model could probably be incorporated in the recently developed automated, bihormonal, bionic pancreas for type 1 diabetes mellitus patients.

INTRODUCTION

In recent years, an increased interest has re-emerged in the role of the glucagon receptor (GCGR) in diabetes and its utility as a therapeutic target [1;2]. In healthy subjects the endocrine pancreas regulates glucose production and metabolism by a synchronized reciprocal release of insulin and glucagon in response to changes in blood glucose levels, free fatty acids (FFA), amino acids, incretin hormones (such as GLP-1 and GIP), among many other signals. In type 2 diabetes mellitus (T2DM), there is evidence for a dysregulation of glucose-insulin-glucagon interaction [3-5]. Elevated fasting and postprandial glucagon concentrations in T2DM patients could suggest a combination of dysregulated glucagon secretion and insulin resistance. The most important consequence of chronic hyperglucagonemia seems to be related to increased glucose production (gluconeogenesis but not glucogenolysis) aggravating hyperglycemia in diabetic patients [6]. Understanding the contribution of glucagon on the glucose metabolism is important for (patho)physiological insight and may also be important in guiding drug development for compounds targeting glucagon.

Glucose metabolism is challenging because of the complex interactions between the hormones involved and the simultaneous effect on glucose in the system. More than 3 decades ago Bergman *et al.* [7] developed the first model for glucose regulation. With help of this model the estimation of glucose tissue uptake sensitivity to insulin levels hypothesis was corroborated in clinical experiments, the biphasic insulin secretion profile was defined and the relationship between insulin and glucose concentrations as a possible mechanism of the disease was suggested.

Basic models in animals and *in vitro* have helped to understand underlying mechanisms and to explore new possible therapeutic targets for diabetes [8-10]. Farhy *et al.* [9] integrated glucagon into the physiological model, creating an explanation of the system from an intercellular level, suggesting high glucagon concentrations as lack of inhibition by glucagon counter regulation in ß-cell deficiency.

Several models based on clinical endpoints in healthy subjects and/or T2DM patients have been developed to describe and better understand the relationship between glucose and insulin [11-17]. PK/PD models have quickly evolved from minimalistic models describing glucose plasma concentrations to complex system pharmacology models that take multiple interactions into account [13;16-19]. Based on earlier models we can describe the general trends between insulin and glucose very well, and find that additional regulators in glucose homeostasis are required to improve our understanding of drug action in healthy volunteers, but more important in diabetes patients. For instance, since 2008 mathematical models of glucagon secretion and glucagon counter regulation based on *in vitro* studies were published [9]. Recently, a semi-mechanistic, integrated glucose-insulin-glucagon model was developed to assess the effects of individualized glucokinase activator on glycemic response [20-22].

However, models incorporating contribution of glucagon to glucose homeostasis while modulating the glucagon receptor, have not been described yet. Therefore we developed a semi-mechanistic model to describe the glucagon-insulin-glucose homeostasis in healthy subjects during a glucagon challenge. Briefly, this challenge consisted of a 3 hrs simultaneous infusion of high glucagon concentrations (supra-physiological) and insulin, while somatostatin was given to block endogenous release of these hormones. The model was subsequently used to predict the influence of the amount of hepatic glucagon receptors in the glucose plasma availability and to perform simulations with hypothetical scenarios for altered glucagon conditions, such as a glucagon challenge.

METHODS

SUBJECTS

Thirty-six healthy male volunteers participated in the clinical study, which was conducted at a single center (CHDR). Their mean (±SD) age was 40.5 ±18.3 years, weight 78.9 ±10.3 kg, body surface area 1.98 ± 0.156 m^2 and body mass index (BMI) 24.0 ±3.1 kg/m^2. Mean fasting glucose and glycosylated hemoglobin A1c baseline values were 5.1 ±0.4 mmol/L and 5.2 ±0.3%, respectively. The protocol was approved by the Central Committee on Research involving Human Subjects of the Netherlands (CCMO). Written consent was obtained from all participants included in the study. The study has already been published [23].

STUDY DESIGN

Subjects were required to continue their normal diet and activities. After an overnight fast, the hyperglucagonemic clamp test was performed, consisting of two phases: a run-in period of 3 hrs to achieve stable glucose isotope enrichment and a 3 hr pancreatic clamp study (Figure 1). After a priming dose of 5 $mg.kg^{-1}$, [6,6-$^2H_2$] glucose was infused continuously throughout the study at a rate of 0.05 $mg.kg^{-1}.min^{-1}$ (Cambridge Isotope Laboratories, MA, USA). The pancreatic clamp study consisted of a simultaneous 3 hrs infusion of somatostatin (0.1 $\mu g.kg^{-1}.min^{-1}$; UCB, The Netherlands), glucagon (3 $ng.kg^{-1}.min^{-1}$; Novo Nordisk, The Netherlands) and insulin (4 $mU.m^{-2}.min^{-1}$; Novo Nordisk, The Netherlands). A second catheter was inserted into a contra-lateral dorsal hand vein for blood sampling. The hand was placed in a heated-box (50°C) to arterialize venous blood for labeled glucose sampling. Venous blood samples were drawn to determine (non-) labeled glucose, glucagon, and insulin concentrations. Samples for isotope analyses, glucose, glucagon and insulin were collected every 15 minutes from 30 minutes before the start of the challenge until the end of the glucagon challenge (t=360 min). After the challenge capillary bedside (finger prick) glucose was measured for informative purposes in 16 subjects at 420, 450 and 480 min.

LABORATORY ANALYSIS

Blood samples for insulin were collected in plain tubes and analyzed using standard validated immune-radio-metric assays (Biosource Europe S.A., Belgium; assay CV 5.9-7.9% for insulin). Glucagon samples were collected in plain tubes with aprotinin (Trasylol™ (500 KIE/50 µl) Bayer, The Netherlands) and analyzed using a radioimmunoassay (Linco research, Missouri, USA; assay CV 4.3%). Blood samples for glucose and [6,6-$^2H_2$] glucose were analyzed using a validated gas chromatography with mass spectrometry as detection method as described previously [24]. All samples were analyzed in batches to reduce assay variability.

MODELING GLUCAGON CHALLENGE

INHIBITION

Somatostatin infusion during the glucagon challenge, which inhibits the endogenous glucagon and insulin secretion, was modeled by an inhibitory function $I_i(t)$ equal to 1, except during the inhibition, when they take on a lower – but still non-negative – value.
The inhibitory functions $I_1(t)$ and $I_3(t)$ in, respectively, equations {4} and {6}, are given by:

$$I_i(t) = 1 - I_{i,max} \times H(t; t_{begin}, t_{end}, \alpha_i), (i = 1,3) \quad \{1\}$$

Where I_{max} denotes the maximal inhibition (i.e., $0 < I_{max} \leq 1$). The function $H(t; t_{start}, t_{end}, \alpha_i)$ denotes a *smooth step function* defined by: {2}

$$H(t; t_{begin}, t_{end}, \alpha_i) = \begin{cases} 0 & \text{for } 0 \leq t \leq t_{begin} \\ 1 - e^{-\alpha_i (t - t_{begin})} & \text{for } t_{begin} < t < t_{end} \\ (1 - e^{-\alpha_i (t_{end} - t_{begin})}) \cdot e^{-\alpha_i (t - t_{end})} & \text{for } t_{end} \leq t < \infty \end{cases}$$

Here $\alpha_i > 0$ is the rate at which the inhibition reaches its maximum value $\approx I_{max}$. The times t_{begin} and t_{end} denote when the inhibitions begin and end.

INFUSIONS

The functions $Q_1(t)$, $Q_2(t)$ and $Q_3(t)$ which model the infusions in, respectively, equations {4}, {5}, and {6}, are given by:

$$Q_i(t) = Q_{i,max} \times \text{Step}(t, T_{begin}, T_{end}), (i = 1, 2, 3) \quad \{3\}$$

Where Step $(t; T_{begin}, T_{end})$, is a simple step-function, which is equal to 1 for $T_{begin} < t < T_{end}$ and 0 elsewhere.

STRUCTURAL MODEL DEVELOPMENT

Using population approach nonlinear mixed effects modeling, glucose-, insulin- and glucagon data from a glucagon challenge in healthy volunteers were simultaneously analyzed. First, the somatostatin effect was modeled as an on-off effect. However, as this led to numerical difficulties in the algorithms, this

was expanded to an inhibitory function (Equation 1). The first-order conditional estimation method with interaction (FOCE I) was used. The log-likelihood ratio test was used to discriminate between hierarchical models, based on the objective function value (OFV), where $p<0.05$ [decrease OFV of at least 3.84 points for one degree of freedom, Chi-square (χ^2) distribution] was considered to be statistically significant. Various goodness-of-fit plots such as: observations vs. population predictions, observations vs. individual predictions, weighted residuals vs. time, (conditional)weighted residuals vs. observed concentrations, histogram and/or QQ plots of the post hoc individual estimates of ETAS (when ETAS were available), population and/or individual predictions vs. observed individual or population concentrations; were considered for diagnostic purposes. Covariate screening was performed by graphical analysis and analysis of the correlation of the post hoc individual estimates of ETA for each parameter versus the covariate values. Three different error types were tested (additional, proportional and both). A model was considered acceptable if the conditional weighted residuals with $\eta-\varepsilon$ interaction (CWRESI) was between -2 and 2. Whenever a new parameter was introduced or the robustness of the model was to be evaluated, the mean population predictions plotted against the observations was performed. The compartmental semi-mechanistic final model structure that best described the observations, including the feedback mechanisms, is illustrated in Figure 2.

GLUCAGON (A_1 IN NANOGRAM)

Glucagon dynamics was described by a turnover equation (Equation 4). The production term (k_{in1}) is taken inversely proportional to the amount of glucose (A_2), as glucagon secretion by α-cells in the pancreas is inhibited by plasma glucose [25;26].

$$\frac{dA_1}{dt} = \frac{k_{in1}}{A_2} \cdot I_1(t) - k_{out1} A_1 + Q_1(t) \quad \{4\}$$

Glucagon elimination was modeled by a first order reaction term with a rate constant k_{out1}, and glucagon infusion was modeled by a function $Q_1(t)$.

PLASMA GLUCOSE (A_2 IN GRAMS)

Glucose dynamics was described by a turnover equation with hepatic glucose production (HGP) and insulin-dependent elimination:

$$\frac{dA_2}{dt} = k_{in2} \frac{A_1}{A_4} - k_{out2} A_2 - k_{out2D} A_2 \cdot A_3 + Q_2(t) \quad \{5\}$$

Glucagon is a potent stimulus of hepatic glucose production, with the magnitude of the effect being dependent on the prevailing insulin concentration;

increasing insulin levels dampen the glucose production [27]. It is known that continuous glucagon infusion results in glucagon receptor internalization (A_4). Intestinal incretin hormones GLP-1 and glucose-dependent insulinotropic polypeptide (GIP) were not included in our model, because all subjects were in a fasting state. Incretin hormones are only released during absorption of orally taken meals and then stimulate pancreatic ß-cells to secrete insulin [28]. Furthermore, the stimulatory effect of autonomic nervous system on hepatic glucose production has not been incorporated in our model, because our previous study showed that changes in the autonomic nervous system tone do not contribute significantly to the effects of the glucagon challenge [23].

Elimination of plasma glucose, which consists of glucose uptake by the liver and muscles is modeled by an insulin independent term ($k_{out2}A_2$) representing e.g. brain glucose consumption and an insulin dependent term ($k_{out2D}A_2 \cdot A_3$) The direct inhibition (negative feedback) of plasma glucose level (A_2) on the liver (HGP) via GLUT-1 transporter is incorporated in the equation as well. Labeled glucose infusion was modeled by a function $Q_2(t)$. Labeled glucose infusion was assumed to have the same disposition properties as total plasma glucose [23;24], therefore no difference in glucose has been made. Labeled glucose and enrichment measurements were not considered in the model.

INSULIN (A_3 IN MILLIUNITS)

Insulin dynamics was described by a turnover equation. Since insulin secretion by ß-cells in the pancreas is stimulated by plasma glucose, the production term is taken proportional to the amount of glucose A_2.
This results in the equation:

$$\frac{dA_3}{dt} = k_{in3} A_2 \cdot I_3(t) - k_{out3} A_3 + Q_3(t) \quad \{6\}$$

Insulin elimination was modeled by a first order elimination process with rate constant k_{out3}, and insulin infusion was modeled by a function $Q_3(t)$, according to equation 3.

INTERNALIZATION OF GLUCAGON RECEPTORS-EFFECT COMPARTMENT (A_4-DIMENSIONLESS)

We observed a rapid increase of the glucose concentration in response to glucagon followed by a slow decrease in the HGP, which is consistent with the internalization of glucagon receptors (GCGR) upon stimulation by glucagon [23;29;30]. Krilov *et al*. [29] have previously shown that, upon 30 minutes of glucagon stimulation, GCGR are internalized in vivo. This internalization of the GCGR was captured by incorporating an effect compartment (A_4). With this we also incorporated a delayed negative effect of hepatic glucose production into

the model (Equation 5). The rate constant of removal from the effect compartment characterized the effect delay.

$$\frac{dA_4}{dt} = k_{in4} A_2 - k_{out4} A_4 \quad \{7\}$$

In the equations 4-7 constitute a coupled system of feedback models: the Glucagon-Glucose system interacting with the Glucose-Insulin system through the effect of hepatic glucose production.

DATA ANALYSIS AND MODEL EVALUATION

The software used for the analysis included: PROMASYS V7.1 (PROMASYS BV, Leiden, The Netherlands) for the database storing and exporting, NONMEM V7.2.0 (Icon Development Solutions, Ellicott City, MD, USA) for the numerical estimations for the established equations [ADVAN 13; tolerance 8], GNU Fortran (GCC) 4.6.0 as compiler and R V2.13.1 (R Foundation for Statistical Computing, Vienna, Austria) for the predictions (simulations), database editing, system solution and graphics elaboration, and MATLAB R2013a (MathWorks, Natick, MA, USA) for simulations.

RESULTS

A semi-mechanistic model simultaneously describing glucagon, plasma glucose, insulin and glucagon receptor internalization, during a hyperglucagonemic challenge was developed. The study cohort investigated in this study covers a broad range of individual data for the model. For each of the 36 subjects, in total 16x glucagon-, 16x glucose- and 16x insulin concentrations before and during the glucagon challenge were measured, and were used for the model. The initial values at steady state for the three compartments were obtained from the first observations (before the challenge was started), the volumes of distribution were obtained from the literature and used as initial estimates [13] and limits were given to values that would be physiological. Also, inter- and intra-individual variability (IIV) was considered but could not be identified given the data.

MODEL EVALUATION / SIMULATIONS

Fitting the model to the data resulted in the following baseline values for glucagon, glucose, insulin and effect compartment:

$$BL_1 = 1170 \text{ ng}, BL_2 = 4.20 \text{ g}, BL_3 = 17.7 \text{ mU}, BL_4 = 4.63 \times 10^6 \quad \{8\}$$

and volumes of distribution of the Glucagon-compartment, the Glucose compartment and the Insulin compartment:

$$V_1 = 21.1 \text{ L}, V_2 = 4.44 \text{ L}, V_3 = 1.53 \text{ L respectively.} \quad \{9\}$$

This results in the following baseline concentrations for the glucagon, plasma glucose and insulin:

$$C_1 = 55.45 \text{ ng/L}, C_2 = 0.946 \text{ g/L}, C_3 = 11.6 \text{ mU/L respectively.} \quad \{10\}$$

The baseline values were used as initial values: $A_i(0) = BL_i$.

Fitting the model to the data yields parameter estimates listed in Table 1, where the values for k_{in1}, k_{in2}, k_{in3} and k_{in4} are computed from the estimated values for k_{out1}, k_{out2}, k_{out2d}, k_{out3} and k_{out4}, and the estimates of the baseline amounts BL_i (i = 1, ...,3) obtained from (Equation 8).

Parameters involved in the glucagon challenge and the infusions are listed in Table 2.

In computing the infusion rates Q_1 and Q_3 in Table 2, we have assumed that the average weight is 80 kg and the average body surface area 1.984 m^2.

Four representative individuals were selected from the whole dataset and are presented in Figure 4. The medians of the simulated individual concentration-time profiles are plotted over the observed profiles of glucose, glucagon and insulin during baseline and during challenge. Individual diagnostic plots for the evaluation of the quality of the model fit, illustrate that the model described the data. During challenge, glucagon data show a decreasing trend, which is captured by the model. As inter- and intra-individual variability could not be identified, the height of the glucagon concentrations could not be captured on an individual level. For plasma glucose concentration during challenge, the increase in glucose levels over time is well captured by the model. There seems to be a slight decreasing trend in glucose concentrations at the end of the challenge, which is better fitted by including the effect compartment (A_4). Even though the fitting is not completely optimal towards the end of the challenge, because it does not describe in some individuals the diminished response to glucagon (glucagon desensitization), inter-individual variability could better explain this phenomenon.

Regarding the recovery phase of plasma glucose levels after challenge, only assumptions were made based on the minor finger prick glucose data points. No laboratory data were collected in the recovery phase.

During challenge a standard insulin dose was infused, and endogenous insulin production was inhibited by somatostatin, therefore insulin concentrations are almost stable during challenge.

However, the predicted insulin concentrations exhibit a peak at the start of the challenge and a drop immediately at the stop of the infusion. These are

artifacts caused by the step function, involving instantaneous onset and termination, while the inhibition of insulin release by somatostatin takes time as does the release of endogenous insulin upon cessation of somatostatin. We decided to not further model this artifact. Firstly, the exact nature of the simultaneously occurring increase in insulin (by the infusion) and the decline in endogenous insulin (by somatostatin) is not very well known. Secondly, the additional parameters required to describe a gradual increase would cause over-parameterization of the model.

In addition to the four representative individuals, Figure 5 shows the diagnostic plots of the entire dataset. It clearly shows that the general trend of all glucagon and glucose data is well captured by the model. The insulin data is also well captured with exception for the peaks at the start and end of the challenge, for reasons mentioned before.

Concentration population predictions vs. conditional weighted residuals graphs for glucagon, glucose and insulin are shown in Figure 6. The glucagon and glucose observations are randomly spread around the identity line and most observations lie within the acceptance criterion. The insulin conditional weighted residuals over time plots show a clear structural bias; the high predicted concentration range is overpredicted (peaks at the start and end of challenge), which is corrected for towards the lower predicted concentration range that, as a result, ends in underpredicted values. The steady state conditions and calculations are supplied in Appendix A.

DISCUSSION

This glucagon receptor (GCGR) modeling approach was a practical tool to describe the glucagon-insulin-glucose homeostasis in healthy subjects during a glucagon challenge [23]. Although this model represents a simplification of complex physiology, the main counter-regulatory elements in the glucose regulation system (glucagon and insulin) were used to describe glucose's profile in a semi-mechanistic way. Application to clinical data showed that the model is able to describe the levels of insulin, glucagon and glucose before and during the glucagon challenge.

Somatostatin was infused during the glucagon challenge to suppress the endogenous hormone production. The model assumed a maximal inhibition (I_{max}) of 1, representing 100% inhibition. Although there is consensus in the literature on the inhibiting effect of somatostatin on endogenous hormone production, the extent of maximal inhibition has not been irrefutably demonstrated. The measured individual glucagon profiles (Figure 4) show a decreasing trend in the glucagon concentrations during the constant glucagon infusion period. The glucagon pattern could be explained by a small reduction of endogenous production on top of the glucagon infusion or the increasing plasma glucose concentration that have an inhibiting effect on the remaining endogenous glucagon excretion.

For the subjects in this study, glucagon levels at baseline were higher when plasma glucose levels were lower. This could be explained by the glucose-dependent regulation of glucagon secretion in the α-cell, as reported in animal studies [26;31]. At low glucose concentrations, the moderate activity of K_{ATP} channels situates the α-cell membrane potential in a range that allows the opening of Na^+ and Ca^{2+}-channels triggering the exocytosis of glucagon granules and vice versa.

The amount of plasma glucose concentrations in this model (Equation 5) is highly dependent on glucagon (A_1) because during the glucagon challenge a supraphysiologic concentration of glucagon was reached. The effect of insulin infusion results in glucose uptake by fat and muscles and a reduction of the supply of gluconeogenic precursors reaching the liver. The data of the study of Sindelar *et al*. [32] strongly suggest that the liver responds directly, rapidly, and sensitively to the plasma insulin levels by a reduction in HGP. The slight decreasing trend in glucose concentrations at the end of the challenge has not been completely captured by the effect compartment (internalization of glucagon receptors). No data were collected for the recovery phase after stopping the glucagon challenge. Therefore, no firm conclusions can be drawn regarding the recovery phase, only assumptions based on the minor finger prick glucose data points.

Insulin and glucagon are fundamental components of the regulator mechanisms that control glucose homeostasis. These counter-regulatory hormones help to keep the blood glucose level within optimum limits. In this work, the insulin, glucagon and glucose interactions following a glucagon challenge have been described in a single model. The adequate descriptive performance of this model has been confirmed by the diagnostic plots per subject and for the total population.

This model, based on glucagon challenge data, could contribute to a better understanding of pathophysiology of diabetes mellitus. It describes the general trend and can therefore serve as a basis for drug development. Furthermore, an extension of this model could probably be incorporated in the recently developed automated, bihormonal, bionic pancreas for type 1 diabetes mellitus patients [33].

APPENDIX A

STEADY STATE AMOUNTS

In the absence of inhibitions and infusions, i.e., when $I_i(t) = 0$ for $i = 1, 3$ and $Q_i(t) = 0$ for $i = 1, 2, 3$ we denote the steady state amounts of the four compounds by $A_{n,ss}$ (n= 1,...,4).

We denote the quotients of k_{in} and k_{out} for each of the four equations by:

$$R_1 = \frac{k_{in1}}{k_{out1}}\ ,\ R_2 = \frac{k_{in2}}{k_{out2}}\ ,\ R_3 = \frac{k_{in3}}{k_{out3}}\ ,\ R_4 = \frac{k_{in4}}{k_{out4}} \qquad \{A.1\}$$

With this notation, $A_{1,ss}$, $A_{3,ss}$ and $A_{4,ss}$ can readily be expressed in terms of $A_{2,ss}$:

$$A_{1,ss} = \frac{R_1}{A_{2,ss}}\ ,\ A_{3,ss} = R_3 A_{2,ss}\ ,\ A_{4,ss} = R_4 A_{2,ss} \qquad \{A.2\}$$

When we substitute these expressions into the right hand side of Equation 5 for dA_2/dt, we obtain an equation for $x = A_{2,ss}$ alone:

$$F(x) \overset{\text{def}}{=} \frac{R_1 \cdot R_2}{R_4} - x^3 - \gamma R_3 \cdot x^4 = 0\ ,\ \gamma = \frac{k_{out2D}}{k_{out2}} \qquad \{A.3\}$$

The function $F(x)$ is seen to have a unique zero: $x = A_{2,ss} = 4.20$. For the parameter values of Table 1, we obtain:

$$R_1 = 4914,\ R_2 = 2.16 \times 10^5,\ R_3 = 4.21,\ R_4 = 1.10 \times 10^6,\ \gamma = 0.650 \qquad \{A.4\}$$

Using these values in the expressions of Equation 5, we obtain for the steady state amounts

$$A_{1,ss} = 1170 \text{ ng},\ A_{2,ss} = 4.20 \text{ g},\ A_{3,ss} = 17.7 \text{ mU},\ A_{4,ss} = 4.63 \times 10^6 \qquad \{A.5\}$$

In the light of the estimated volumes, given in Equation 9, the corresponding steady state concentrations are:

$$C_{1,ss} = 55.45 \text{ ng/L},\ C_{2,ss} = 0.946 \text{ g/L},\ C_{3,ss} = 11.6 \text{ mU/L} \qquad \{A.6\}$$

TABLE 1 Parameter estimates for glucagon, plasma glucose, insulin, glucagon receptor internalization and volume of distribution. Parameters with an asterix denote calculated parameters (not directly estimated by NONMEM).

Parameter	Estimate	Unit
k_{in1}	559*	$ng \cdot g \cdot min^{-1}$
k_{out1}	0.114	min^{-1}
k_{in2}	275*	$g \cdot (ng \cdot min)^{-1}$
k_{out2}	0.00127	$(mU \cdot min)^{-1}$
k_{out2D}	8.26×10^{-4}	min^{-1}
k_{in3}	2.09*	$mU \cdot (g \cdot min)^{-1}$
k_{out3}	0.496	min^{-1}
k_{in4}	655*	$(g \cdot min)^{-1}$
k_{out4}	5.94×10^{-4}	min^{-1}

TABLE 2 Parameter values involved in glucagon challenge and infusions.

Parameter	Estimate	Unit
α_1	7.00×10^{-4}	min^{-1}
α_3	1.18×10^{-1}	min^{-1}
Q_1*	240	$ng \cdot min^{-1}$
Q_2(5 min bolus)*	0.001	$g \cdot kg^{-1}$
Q_2*	0.00001	$g \cdot kg^{-1} \cdot min^{-1}$
Q_3*	7.936	$mU \cdot min^{-1}$

** fixed parameters*

FIGURE 1 Glucagon challenge; infusion of somatostatin, glucagon, insulin and labeled glucose.

Basal period		Hyperglucagonaemic period
0 min - - - 5 min	5 min - - - 180 min	180min - - - 360 min
[6.6'-2H2] glucose bolus 5 $mg.kg^{-1}$	[6.6'-2H2] glucose continuous 0.05 $mg.kg^{-1}.min^{-1}$	
		Somatostatin 0.1 $\mu g.kg^{-1}.min^{-1}$
		Glucagon 3 $ng.kg^{-1}.min^{-1}$
		Insulin 4 $mU.m^{-2}.min^{-1}$

FIGURE 2 Schematic representation of the model. Full arrows indicate flows, broken arrows indicate control mechanisms, dotted arrows indicate infusion of somatostatin, glucagon, insulin and labeled glucose.

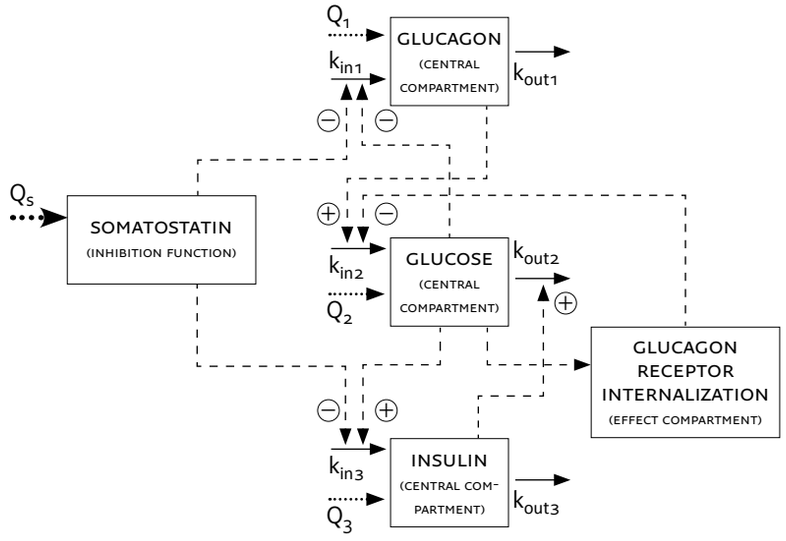

FIGURE 3 The inhibition functions $I_1(t)$, with $\alpha = 0.0007$, and $I_3(t)$, with $\alpha = 0.118$, for $t_{begin} = 5$ and $t_{end} = 180$ min.

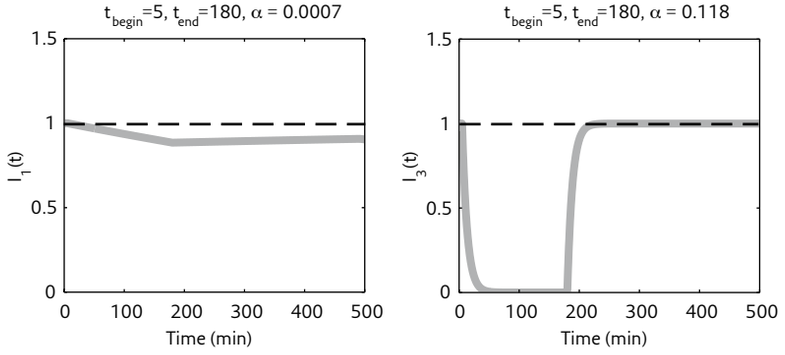

FIGURE 4 Representative profiles for glucagon, glucose and insulin of four typical healthy subjects. Observations from the original data set are plotted as points. The lines show the average predicted values of the model. The vertical dashed lines represent the time of start and stop of the glucagon challenge test.

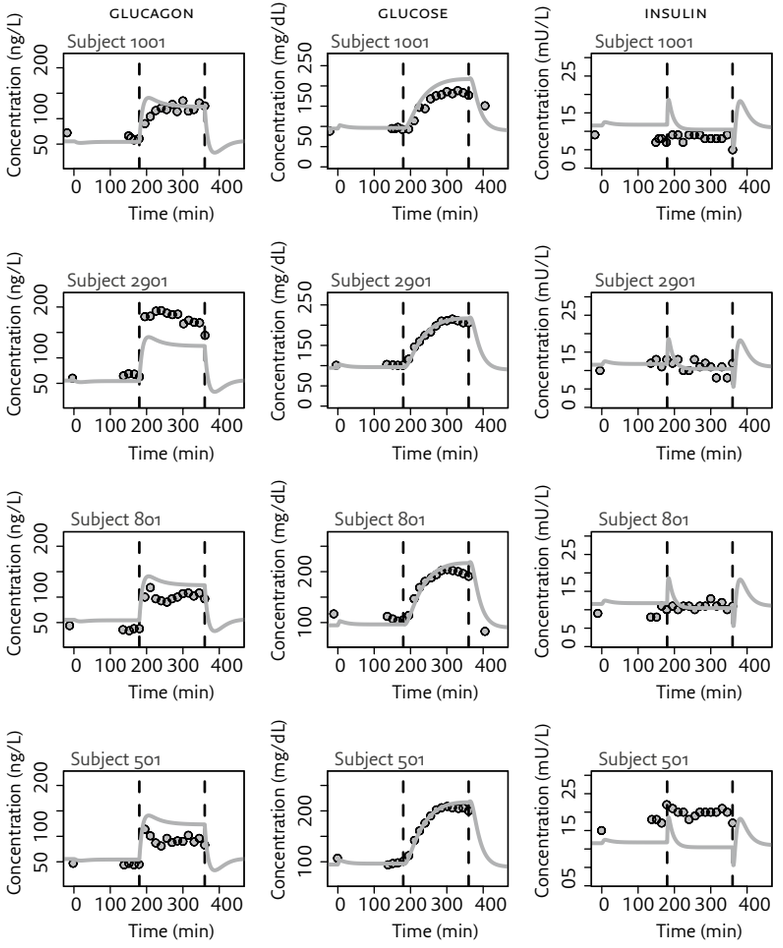

FIGURE 5 Diagnostic plots representing the mean population prediction (black) over time for glucagon, plasma glucose and insulin, with the observations (circles).The vertical dashed lines represent the time of start and stop of the glucagon challenge test.

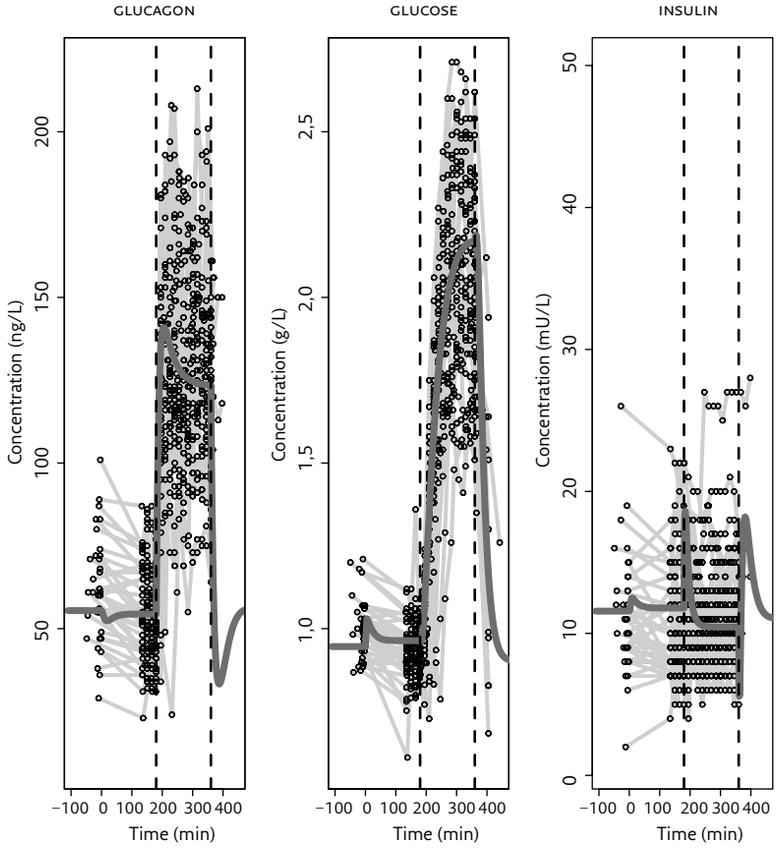

FIGURE 6 Glucose, glucagon and insulin conditional weighted residuals graphed versus predicted population concentrations. Data points are plotted as circles. The horizontal line is the identity line at zero and the dotted line represents the acceptance criterion.

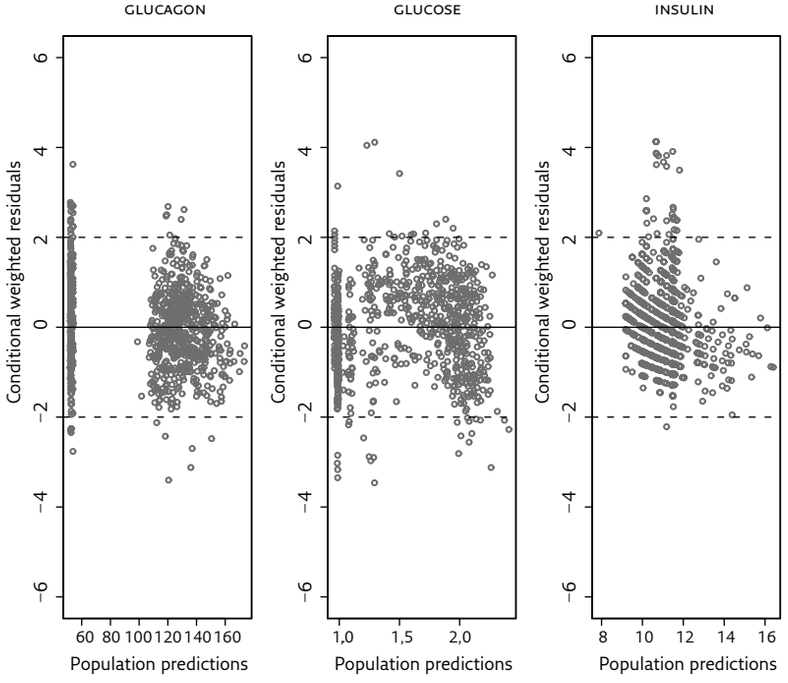

REFERENCES

1 Petersen KF, Sullivan JT: Effects of a novel glucagon receptor antagonist (Bay 27-9955) on glucagon-stimulated glucose production in humans. Diabetologia 2001;44:2018-2024.
2 Sloop KW, Michael MD, Moyers JS: Glucagon as a target for the treatment of Type 2 diabetes. Expert Opin Ther Targets 2005;9:593-600.
3 Dinneen S, Alzaid A, Turk D, Rizza R: Failure of glucagon suppression contributes to postprandial hyperglycemia in IDDM. Diabetologia 1995;38:337-343.
4 Dunning BE, Gerich JE: The role of alpha-cell dysregulation in fasting and postprandial hyperglycemia in type 2 diabetes and therapeutic implications. Endocr Rev 2007;28:253-283.
5 Unger RH: Letter: Glucagon in pathogenesis of diabetes. Lancet 1975;1:1036-2.
6 Matsuda M, Defronzo RA, Glass L, Consoli A, Giordano M, Bressler P, Delprato S: Glucagon dose-response curve for hepatic glucose production and glucose disposal in type 2 diabetic patients and normal individuals. Metabolism 2002;51:1111-1119.
7 Bergman RN, Ider YZ, Bowden CR, Cobelli C: Quantitative estimation of insulin sensitivity. Am J Physiol 1979;236:E667-E677.
8 Chew YH, Shia YL, Lee CT, Majid FA, Chua LS, Sarmidi MR, Aziz RA: Modeling of glucose regulation and insulin-signaling pathways. Mol Cell Endocrinol 2009;303:13-24.
9 Farhy LS, McCall AL: Models of glucagon secretion, their application to the analysis of the defects in glucagon counterregulation and potential extension to approximate glucagon action. J Diabetes Sci Technol 2010;4:1345-1356.
10 Liu W, Tang F: Modeling a simplified regulatory system of blood glucose at molecular levels. J Theor Biol 2008;252:608-620.
11 Cobelli C, Pacini G: Insulin secretion and hepatic extraction in humans by minimal modeling of C-peptide and insulin kinetics. Diabetes 1988;37:223-231.
12 De GA, Arino O: Mathematical modelling of the intravenous glucose tolerance test. J Math Biol 2000;40:136-168.
13 Jauslin PM, Silber HE, Frey N, Gieschke R, Simonsson US, Jorga K, Karlsson MO: An integrated glucose-insulin model to describe oral glucose tolerance test data in type 2 diabetics. J Clin Pharmacol 2007;47:1244-1255.
14 Landersdorfer CB, Jusko WJ: Pharmacokinetic/pharmacodynamic modelling in diabetes mellitus. Clin Pharmacokinet 2008;47:417-448.
15 Ruggiero C, Giacomini M, Gaglio S: A qualitative model of the dynamics of blood glucose and its hormonal control. Comput Methods Programs Biomed 1993;40:117-130.
16 Silber HE, Jauslin PM, Frey N, Gieschke R, Simonsson US, Karlsson MO: An integrated model for glucose and insulin regulation in healthy volunteers and type 2 diabetic patients following intravenous glucose provocations. J Clin Pharmacol 2007;47:1159-1171.
17 Silber HE, Frey N, Karlsson MO: An integrated glucose-insulin model to describe oral glucose tolerance test data in healthy volunteers. J Clin Pharmacol 2010;50:246-256.
18 Dahl SG, Aarons L, Gundert-Remy U, Karlsson MO, Schneider YJ, Steimer JL, Troconiz IF: Incorporating physiological and biochemical mechanisms into pharmacokinetic-pharmacodynamic models: a conceptual framework. Basic Clin Pharmacol Toxicol 2010;106:2-12.
19 Jauslin PM, Frey N, Karlsson MO: Modeling of 24-hour glucose and insulin profiles of patients with type 2 diabetes. J Clin Pharmacol 2011;51:153-164.
20 Schaller S, Willmann S, Lippert J, Schaupp L, Pieber TR, Schuppert A, Eissing T: A Generic Integrated Physiologically based Whole-body Model of the Glucose-Insulin-Glucagon Regulatory System. CPT Pharmacometrics Syst Pharmacol 2013;2:e65.
21 Schneck KB, Zhang X, Bauer R, Karlsson MO, Sinha VP: Assessment of glycemic response to an oral glucokinase activator in a proof of concept study: application of a semi-mechanistic, integrated glucose-insulin-glucagon model. J Pharmacokinet Pharmacodyn 2013;40:67-80.
22 Zhang X, Schneck K, Bue-Valleskey J, Yeo KP, Heathman M, Sinha V: Dose selection using a semi-mechanistic integrated glucose-insulin-glucagon model: designing phase 2 trials for a novel oral glucokinase activator. J Pharmacokinet Pharmacodyn 2013;40:53-65.
23 van Dongen MG, Geerts BF, Bhanot S, Morgan ES, de Kam ML, Moerland M, Romijn JA, Cohen AF, Burggraaf J: Characterization of a standardized glucagon challenge test as a pharmacodynamic tool in pharmacological research. Horm Metab Res 2014;46:269-273.
24 Reinauer H, Gries FA, Hubinger A, Knode O, Severing K, Susanto F: Determination of glucose turnover and glucose oxidation rates in man with stable isotope tracers. J Clin Chem Clin Biochem 1990;28:505-511.
25 MacDonald PE, De Marinis YZ, Ramracheya R, Salehi A, Ma X, Johnson PR, Cox R, Eliasson L, Rorsman P: A K ATP channel-dependent pathway within alpha cells regulates glucagon release from both rodent and human islets of Langerhans. PLoS Biol 2007;5:e143.
26 Quesada I, Tuduri E, Ripoll C, Nadal A: Physiology of the pancreatic alpha-cell and glucagon secretion: role in glucose homeostasis and diabetes. J Endocrinol 2008;199:5-19.
27 Shah P, Basu A, Basu R, Rizza R: Impact of lack of suppression of glucagon on glucose tolerance in humans. Am J Physiol 1999;277:E283-E290.
28 Drucker DJ, Nauck MA: The incretin system: glucagon-like peptide-1 receptor agonists and dipeptidyl peptidase-4 inhibitors in type 2 diabetes. Lancet 2006;368:1696-1705.
29 Krilov L, Nguyen A, Miyazaki T, Unson CG, Williams R, Lee NH, Ceryak S, Bouscarel B: Dual mode of glucagon receptor internalization: role of PKCalpha, GRKs and beta-arrestins. Exp Cell Res 2011;317:2981-2994.
30 Merlen C, Fabrega S, Desbuquois B, Unson CG, Authier F: Glucagon-mediated internalization of serine-phosphorylated glucagon receptor and Gsalpha in rat liver. FEBS Lett 2006;580:5697-5704.
31 Vieira E, Salehi A, Gylfe E: Glucose inhibits glucagon secretion by a direct effect on mouse pancreatic alpha cells. Diabetologia 2007;50:370-379.
32 Sindelar DK, Chu CA, Venson P, Donahue EP, Neal DW, CherrinGTon AD: Basal hepatic glucose production is regulated by the portal vein insulin concentration. Diabetes 1998;47:523-529.
33 Russell SJ, El-Khatib FH, Sinha M, Magyar KL, McKeon K, Goergen LG, Balliro C, Hillard MA, Nathan DM, Damiano ER: Outpatient glycemic control with a bionic pancreas in type 1 diabetes. N Engl J Med 2014;371:313-325.

CHAPTER 7

Summary and general discussion